9-1-1998

Maintenance of Circulation Anomalies during the 1988 Drought and 1993 Floods over the United States

Alan Z. Liu
Embry Riddle Aeronautical University - Daytona Beach, liuz2@erau.edu

Mingfang Ting

Hailan Wang

Maintenance of Circulation Anomalies during the 1988 Drought and 1993 Floods over the United States

ALAN Z. LIU,* MINGFANG TING, AND HAILAN WANG

Department of Atmospheric Sciences, University of Illinois at Urbana-Champaign, Urbana, Illinois

(Manuscript received 10 February 1997, in final form 7 January 1998)

ABSTRACT

The large-scale circulation anomalies associated with the 1988 drought and the 1993 floods are investigated with the National Centers for Environmental Prediction Reanalysis data and a linear stationary wave model. The transient vorticity and thermal forcings are explicitly calculated and the diabatic heating is derived as a residual in the thermodynamic energy equation. Using the April–June (AMJ) data for 1988, and June–August (JJA) data for 1993, the linear stationary wave model is able to reproduce the main features of the geopotential height anomaly for the two seasons when all forcings are included. This provides a basis for further investigation of stationary wave response to different forcing mechanisms using the linear model.

Within the linear model framework, the linear model responses to different forcings are examined separately. The results indicate that the 1988 anomaly over the United States is a result of both the diabatic heating and the transient vorticity and thermal forcings. The large anticyclonic anomalies over the North Pacific and Canada are forced mainly by the diabatic heating. The 1993 anomaly, however, is dominated by the response to transient vorticity forcing. By further separating the linear model responses to regional diabatic heating anomalies in 1988, the results indicate that the western North Pacific heating is entirely responsible for the anticyclonic center over the North Pacific, which causes the northward shift and intensification of the Pacific jet stream. The eastern North Pacific heating/cooling couplet is the most important for maintaining the North American circulation anomaly. The tropical eastern Pacific cooling/heating anomalies associated with the La Niña condition have negligible influence on the North American circulation. In 1993, the strong diabatic heating over the North American continent largely compensates the effect of the cooling over the North Pacific.

The dynamics of the AMJ and JJA climate is further explored by calculating its Green's function for both diabatic heating and vorticity forcing. The results again show negligible influence from the equatorial Pacific. The most effective location for diabatic heating to generate a North American circulation anomaly is along the west coast of North America, where the zonal wind is relatively weak. There is little sensitivity in the Green's function solution to the different basic states.

1. Introduction

Warm season precipitation over the United States varies greatly from year to year (Ting and Wang 1997). For example, the 1988 drought over most of the continental United States and the 1993 floods over the Mississippi River basin are two extreme manifestations of the precipitation variations. Although precipitation amount can be affected by many factors, such as the moisture availability, soil wetness, and frequency of storm activity, very large and persistent precipitation anomalies are often associated with extreme atmospheric circulation anomalies. The large-scale circulation pattern determines the location and intensity of the storm tracks, as well as the directions of horizontal moisture transports.

Large-scale circulation anomalies were observed over the North Pacific and North America during the spring of 1988 and summer of 1993 (NOAA 1988, 1993). These are accompanied by anomalous conditions in both the diabatic heating and the transient wave activity. Using a baroclinic steady-state model linearized about the April–June (AMJ) climate, Trenberth and Branstator (1992) showed that an anomalous heat source located in the subtropical eastern Pacific was able to produce a wave train that is similar to the observed stationary wave anomalies in 1988. The heating anomaly over the subtropical eastern Pacific is further linked to the anomalously cold sea surface temperature (SST) in this region. For the 1993 floods, Trenberth and Guillemot (1996) again linked the extratropical circulation anomaly to the tropical heating anomaly associated with warm SST conditions over the tropical Pacific.

* Current affiliation: Department of Electrical and Computer Engineering, University of Illinois at Urbana-Champaign, Urbana, Illinois.

Corresponding author address: Dr. Alan Z. Liu, 308 CSRL, 1308 West Main St., University of Illinois at Urbana-Champaign, Urbana, Illinois 61801.
E-mail: liuzr@uiuc.edu

In addition to tropical SST anomalies, large North Pacific SST anomalies were also present (NOAA 1988, 1993) in both the 1988 and 1993 events. Some studies have shown that the North Pacific SST anomaly may also be related to the atmospheric circulation anomalies. Wallace and Jiang (1987) found significant correlations between atmospheric circulation anomalies and the North Pacific SST anomalies. Ting and Wang (1997) found high correlations between the summertime U.S. precipitation anomalies and the Pacific SST anomalies, and the correlation is larger over the North Pacific than over the tropical Pacific. How the North Pacific SST influences the extratropical circulation, on the other hand, is still not well understood.

Transient eddies could also be responsible for the circulation anomalies. In the summer of 1993, transient eddies played an important role in strengthening the jet over the Pacific and maintaining a lee trough downstream of the Rockies, therefore maintaining the flood pattern (Mo et al. 1995). The weakening (strengthening) of the midlatitude storm activity during the 1988 drought (1993 floods) over the United States has also been noted by Trenberth and Guillemot (1996). Due to the complexity of the dynamical and physical processes involved, it is necessary to quantify the relative importance of the various forcing mechanisms for the maintenance of the large-scale circulation anomaly observed in the 1988 drought and 1993 floods.

Our approach is to diagnose the stationary wave anomalies through the use of a linear stationary wave model. This model has been used widely in diagnosing the maintenance mechanisms of the anomalous stationary waves in winter (e.g., Ting and Held 1990; Branstator 1992) among others. For the spring and summer, however, the linear stationary wave model is not as widely used. In this study, we linearize the model about *observed* three-dimensional AMJ and June–August (JJA) climatological states, and investigate the linear stationary wave dynamics in response to various forcings. We try to address the following questions:

- Can a linear stationary wave model reproduce the observed stationary wave anomalies in 1988 and 1993, with realistic forcing and realistic climatological basic state?
- What is the relative importance of different forcings, including transients and diabatic heating, in the maintenance of the stationary wave anomaly?
- In what regions were the forcings most effective in producing the observed anomalies over North America?

Our linear modeling approach is similar to Trenberth and Branstator (1992). The most important difference is that the linear model is used as a diagnostic tool in this study, whereas it is a mechanistic model in Trenberth and Branstator. The advantage of using the linear model as a diagnostic tool is that not only the spatial pattern but the amplitude of the response to each forcing mechanism can be determined. While the spatial structure of the atmospheric response to the subtropical eastern Pacific heating is similar to the observed anomalies in 1988, it may not be a significant contribution toward the total atmospheric anomalies if the amplitude is small compared to observations. Other improvements in this study include an increased horizontal and vertical resolutions (full rhomboidal 15, 14 σ levels) and a high quality dataset from the National Centers for Environmental Prediction (NCEP) Reanalysis.

This paper is organized as follows. In the next section, the steady linear baroclinic model is briefly described, together with the data and method we use to calculate the forcings. In section 3, observed features of the stationary waves and the anomalous forcings in 1988 and 1993 are discussed. In section 4 we present the model-simulated stationary waves and their comparison with observations, followed by the decomposition of the response for each individual forcing and in different regions to examine their relative contributions. In section 5, we present the results with the calculation of the Green's function to determine the most effective region for the forcing to generate the observed stationary wave anomaly. Finally, a summary is given in section 6.

2. Data and methods

a. Dataset

The basic dataset used in this study is the NCEP Reanalysis for a nine-year period from 1985 to 1993. The reanalysis data is produced by a fixed, state-of-the-art global data assimilation system (Kalnay et al. 1996). It is therefore free from data inconsistency due to the change of assimilation system. The consistency is particularly important for studying the interannual variability and makes the dataset well suited for the budget calculation used here. The original data has a spatial resolution of 2.5° in both longitudinal and latitudinal directions, and 17 pressure levels up to 10 hPa. The temporal resolution of the original dataset is four times daily. We reduced it to twice daily in our calculation to speed up data processing. We found no noticeable difference in the transient flux fields due to this reduction. The variables used in the calculation include three-dimensional wind, temperature, geopotential height, and surface pressure. We calculated horizontal vorticity fluxes, horizontal divergence fluxes, and horizontal and vertical heat fluxes using the twice daily data on original spatial resolutions. The diabatic heating is then diagnosed as a residual from the thermodynamic equation. These data are subsequently interpolated into R15 resolution and 14 σ levels to be incorporated into the linear model. The long-term mean climatology of all the fields is defined as the nine-year average and the seasonal mean anomalies as deviation of seasonal mean of an individual year from the long-term mean climatology.

b. Linear stationary wave model

The linear stationary wave model was developed by Ting and Held (1990) and was used to diagnose the stationary wave response to a tropical SST anomaly in an idealized general circulation model (GCM). It has been successfully used to diagnose the maintenance mechanisms of the summertime climatological stationary waves in a GCM (Ting 1994).

The basic equations include four prognostic equations for vorticity, divergence, temperature, and log surface pressure, and two diagnostic equations describing the mass continuity and the hydrostatic balance. In this model, the time tendencies are set to zero and the atmospheric response to a given forcing is calculated by solving a set of linear equations. The coefficients of this set of equations are determined by the basic state as well as dissipation. The details of the model are described in Ting (1994) and Ting and Held (1990).

In this study we use a full R15 resolution in the horizontal and 14 σ levels in the vertical with unevenly distributed σ values (0.015, 0.05, 0.101, 0.171, 0.257, 0.355, 0.46, 0.568, 0.676, 0.777, 0.866, 0.935, 0.979, 0.997). We define the basic state as the three-month-mean (AMJ or JJA) climatology based on the nine-year reanalysis data from 1985 to 1993. The forcings that generate the stationary wave anomaly include the diabatic heating and the transient forcing. In addition, the nonlinear terms omitted in the linearization of the governing equations are also included as a forcing. All transient forcings are calculated for submonthly timescales. The anomalous diabatic heating and transient forcing for AMJ 1988 and JJA 1993 are obtained as departures of the three-month-average from the corresponding 9-yr (1985–93) climatology. The nonlinear terms are calculated based on the observed stationary wave anomalies in AMJ of 1988 and JJA of 1993, respectively.

Several dissipative parameterizations are included in this model to ensure a meaningful steady-state solution. These include Rayleigh friction, Newtonian damping, and a biharmonic diffusion in the vorticity, divergence, and thermodynamic equations. They can be expressed as follows:

$$\frac{\partial \zeta}{\partial t} = \ldots - \kappa\zeta - \upsilon\nabla^4\zeta$$

$$\frac{\partial D}{\partial t} = \ldots - \kappa D - \upsilon\nabla^4 D$$

$$\frac{\partial T}{\partial t} = \ldots - (\kappa + \upsilon\nabla^4)\left(T - \frac{\partial [T]}{\partial \ln\sigma}\ln p_s\right),$$

where the Rayleigh friction and Newtonian damping coefficients are chosen to be

$$\kappa = \begin{cases} (0.25\ \text{day})^{-1}, & \sigma = 0.997 \\ (0.5\ \text{day})^{-1}, & \sigma = 0.979 \\ (1.5\ \text{day})^{-1}, & \sigma = 0.935 \\ (15\ \text{day})^{-1}, & \text{elsewhere.} \end{cases}$$

The biharmonic diffusion is highly scale selective with a coefficient of $\nu = 1 \times 10^{17}\ \text{m}^4\ \text{s}^{-1}$, corresponding to an *e*-folding time of 5.3 h for the smallest scale resolved in the model.

The model calculates only the response of the zonally asymmetric components. In other words, zonal-mean anomalies generated by zonal-mean forcings are not included. The effects of the variability of the zonal-mean flow on the stationary waves for the winter season are studied in Hoerling et al. (1995) and Ting et al. (1996), but are beyond the scope of this study. The model response is interpolated to pressure levels for easy comparison with observations.

c. Green's function approach

To further explore the dynamical property of the basic state, we calculated its Green's function. The amplitude and distribution of the Green's function for a given reference point represents the relative effectiveness of the forcings in exciting the stationary wave anomalies at the reference point. This method was used by Branstator (1985) in his study of the linear response to tropical SST anomaly in a barotropic model. In this study, the Green's function is separately calculated for the diabatic heating and the vorticity forcing. Since our interest is primarily in the horizontal structures of the forcing and the response, the forcing is specified as nonzero in a vertical column at a horizontal grid and zero everywhere else. The vertical distribution of the forcing in the column is specified with a vertical profile. The formula for the Green's function can be symbolically written as:

$$\mathbf{L}G(\lambda, \phi, \sigma; \lambda_0, \phi_0) = \delta(\lambda_0, \phi_0)h(\sigma),$$

where $\mathbf{L}$ is a three-dimensional linear operator determined by the basic state and dissipations, $\delta(\lambda_0, \phi_0)$ is a forcing function that is nonzero only at longitude λ_0 and latitude ϕ_0, $h(\sigma)$ is a vertical profile, $G(\lambda, \phi, \sigma; \lambda_0, \phi_0)$ is the response at longitude λ and latitude ϕ, namely, the Green's function; G can be calculated for all (λ_0, ϕ_0) in the entire domain. Given a particular point of interest $(\lambda^*, \phi^*, \sigma^*)$, we can then plot contours of $G(\lambda^*, \phi^*, \sigma^*, \lambda_0, \phi_0)$ for all (λ_0, ϕ_0). The distribution of G is a measure of sensitivity of the model response due to forcing at different regions. More detailed explanation of the Green's function calculation will be presented in section 5.

3. Observational features

In this section, we present the observational features of the AMJ and JJA climate and the stationary wave anomalies for 1988 and 1993, respectively. The diabatic heating and transient forcings for the two seasons derived from the NCEP Reanalysis will also be presented. The validity of the derived forcing fields will be examined. Since our primary interest is in the Pacific and North American region, all diagrams are shown for the

region between 120°E and 60°W and between the equator and the North Pole, even though all analyses and model experiments are performed on the whole globe.

a. Mean climate

The AMJ and JJA climate states are shown in Fig. 1 for the 200-hPa zonally asymmetric component of the geopotential height Z and the zonal wind component. The climatological stationary waves in AMJ (Fig. 1a) and JJA (Fig. 1b) share some familiar features, such as the dominant anticyclonic circulation over the U.S. continent and the cyclonic centers off the tip of the Aleutians over the North Pacific and off the U.S. West Coast over the subtropical Pacific. The most important difference in climatology between the two seasons is the stronger and more eastward extended jet stream over the Pacific in late spring (Fig. 1c) compared to the summer (Fig. 1d). The easterlies in the Tropics cover the whole Pacific in the summer, with amplitude over 10 m s^{-1} in the eastern and western tropical Pacific. In AMJ, however, the tropical easterlies cover only the eastern and western Pacific basins and in the central equatorial Pacific weak westerlies prevail. The strong easterlies in the summer prevent waves generated in the Tropics from propagating into midlatitudes, and can have a strong impact on the response of stationary waves in the model.

b. Stationary wave anomalies

The observed stationary wave anomaly in AMJ 1988 is depicted by the zonally asymmetric component of Z in Fig. 2. The horizontal structure of the 200-hPa geopotential height anomalies (Fig. 2a) show a well-defined wavelike pattern over the Pacific and North American region. This wavelike pattern consists of an anticyclonic center over the central Pacific, a low over the Gulf of Alaska, another high over the Northern half of the United States and most of the Canada, and a low center over the southeast of the United States. This wavelike structure led Trenberth and Branstator (1992) to speculate on the possible role of the tropical heating anomalies associated with La Niña. The amplitudes of the anomaly centers in Fig. 2a are comparable to the climatological stationary waves at the same location. Compared to Fig. 1a, the stationary waves in 1988 are an intensification of the climatological stationary waves north of 40°N.

The vertical structure of the stationary wave anomaly in midlatitudes is depicted in Fig. 2b by a longitude–vertical cross section at 50°N, which is close to the maximum centers in Fig. 2a. The vertical structure of the stationary wave anomaly is largely equivalent barotropic, with no change of sign throughout the vertical column. Because of the equivalent barotropic structure, the 200-hPa Z is a good representation of the overall structure of the stationary wave anomalies.

The 1993 summer stationary wave anomaly is shown in Fig. 3. North of 30°N, a succession of lows and highs spans the North Pacific and North American region: two lows over the central North Pacific and western North America, and two highs over the northwestern Pacific and the east coast of North America, respectively. The anomalies are of smaller zonal scale and shifted slightly southward compared to the 1988 anomalies. The sign of the height anomaly over North America is almost reversed for the two seasons, with 1988 dominated by an anticyclone and 1993 by a cyclone. The different signs of the height anomaly over North America seem to be strongly associated with the drought and floods that occurred during the two seasons.

The vertical structure of the 1993 anomaly at 45°N is shown in Fig. 3b. Similar to 1988, the height anomaly is equivalent barotropic, with maximum amplitudes located between 200 and 300 hPa.

c. Anomalous diabatic heating

The vertically integrated diabatic heating anomalies as derived from the NCEP Reanalysis for AMJ 1988 and JJA 1993 are shown in Fig. 4. In AMJ 1988 (Fig. 4a), the dominant feature is a broad band of cooling equatorward of 10°N across the whole Pacific. It is associated with below normal SST in the region. Farther north of the cooling region, there is anomalous heating in the eastern Pacific at about 15°–20°N. Large heating centers are also found along the west coast of North America from California to Canada, over Alaska, and over the western North Pacific. There is weak cooling over the United States associated with the drought condition.

In JJA 1993 (Fig. 4b), there is mostly positive heating over the tropical Pacific, as well as over most of the United States, in contrast to those in 1988. The positive heating anomaly over the tropical Pacific is related to the weak El Niño condition and that over North America to the floods. The cooling regions to the west coast of North America in Fig. 4b also seem to contrast with the heating in Fig. 4a. Overall, the diabatic heating anomalies during summer 1993 shows the opposite sign to that in 1988 over most of the regions.

The diabatic heating shown in Fig. 4 is derived as a residual from the thermodynamic equation. To verify the validity of the derived heating anomalies for the two seasons, the corresponding observed outgoing longwave radiation (OLR) is shown in Fig. 5. A positive (negative) OLR anomaly indicates reduced (enhanced) convective activities, and should correspond to a negative (positive) diabatic heating anomaly. The correspondence between the derived heating in Fig. 4 and the corresponding OLR is generally good in the Tropics, where most diabatic heating comes from deep convection. In midlatitudes, shallow convection also releases a significant amount of latent heat, while it may not show large signals in the OLR. Thus, the correspondence between the OLR and the diabatic heating in midlatitudes is not as good as in the Trop-

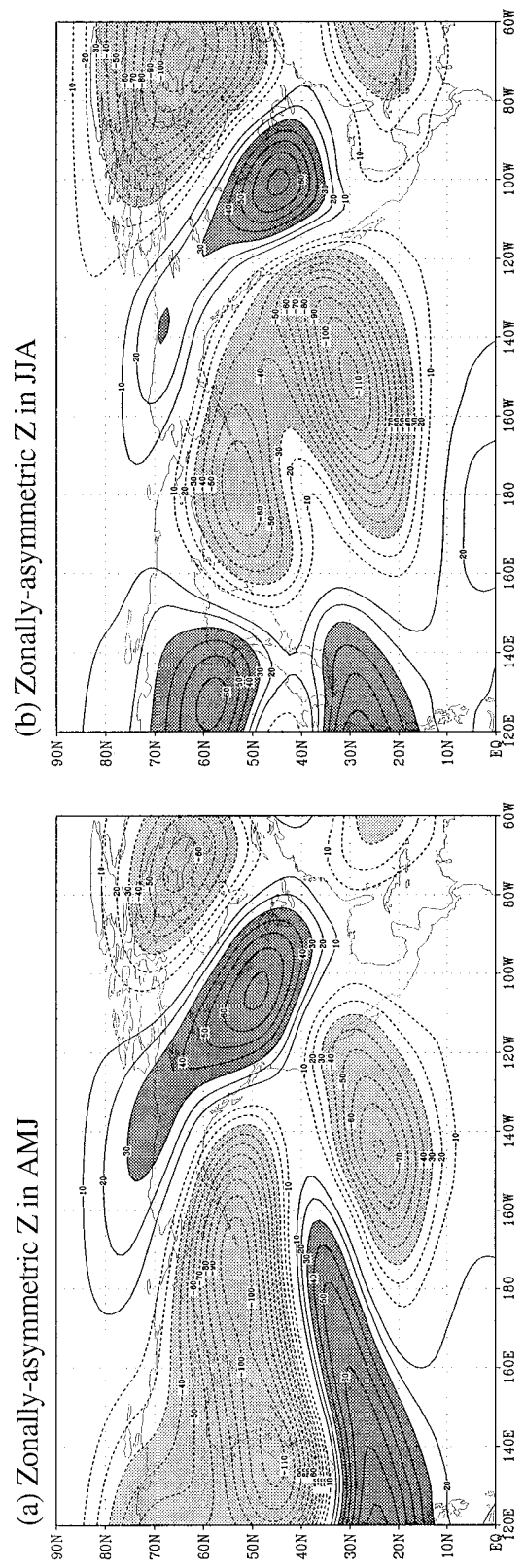

FIG. 1. Observed AMJ and JJA climate at 200 hPa. (a) and (b) Zonally asymmetric Z in AMJ and JJA, respectively: CI = 10 m; Dark-shaded areas are $Z > 30$ m and lightly shaded areas are $Z < -30$ m. (c) and (d) Zonal wind in AMJ and JJA, respectively: CI = 5 m s^{-1}. Shaded regions are easterlies.

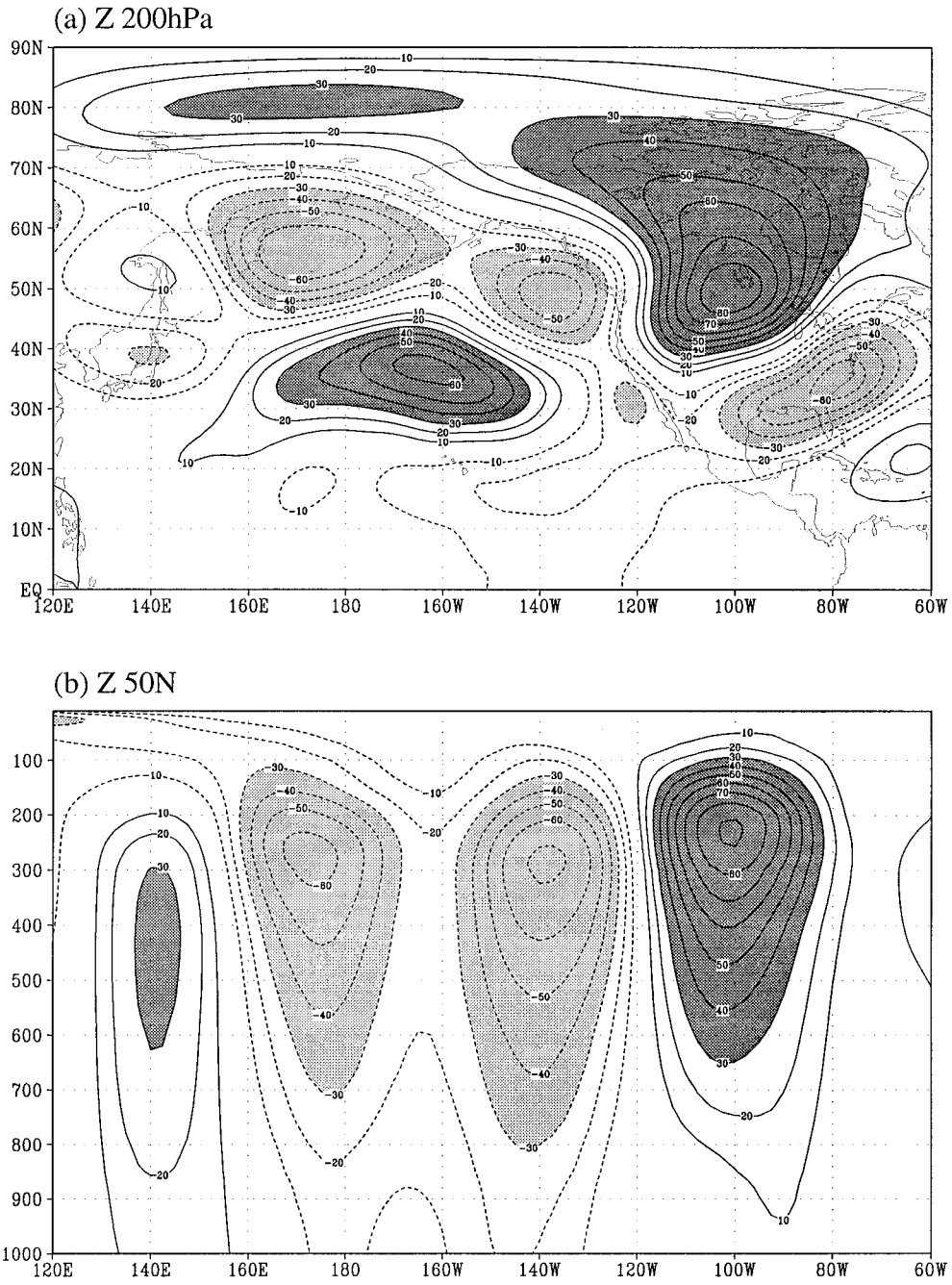

FIG. 2. Observed zonally asymmetric Z anomaly in AMJ 1988: (a) horizontal distribution at 200 hPa and (b) Vertical–longitude cross section at 50°N; CI = 10 m. Areas above 30 m are dark shaded and areas below −30 m are lightly shaded.

ics. Nevertheless, most of the features present in the derived heating fields can find their counterparts in the OLR. The most noteworthy difference is the smaller amplitude in derived cooling in 1988 and a southeastward shift in derived heating in 1993 over the United States compared to OLR. The weaker derived U.S. cooling in AMJ 1988 indicates deficiencies of the reanalysis data, whereas the derived U.S. heating in 1993 corresponds better with the actual precipitation (Fig. 4 in Kunkel et al. 1994) than OLR. There are many other detailed differences between derived heating and OLR over the Pacific region, but the qualitative agreement is reasonable. Due to the lack of a high quality three-dimensional diabatic heating dataset, the derived diabatic heating will be used in the linear model calculations in the next section.

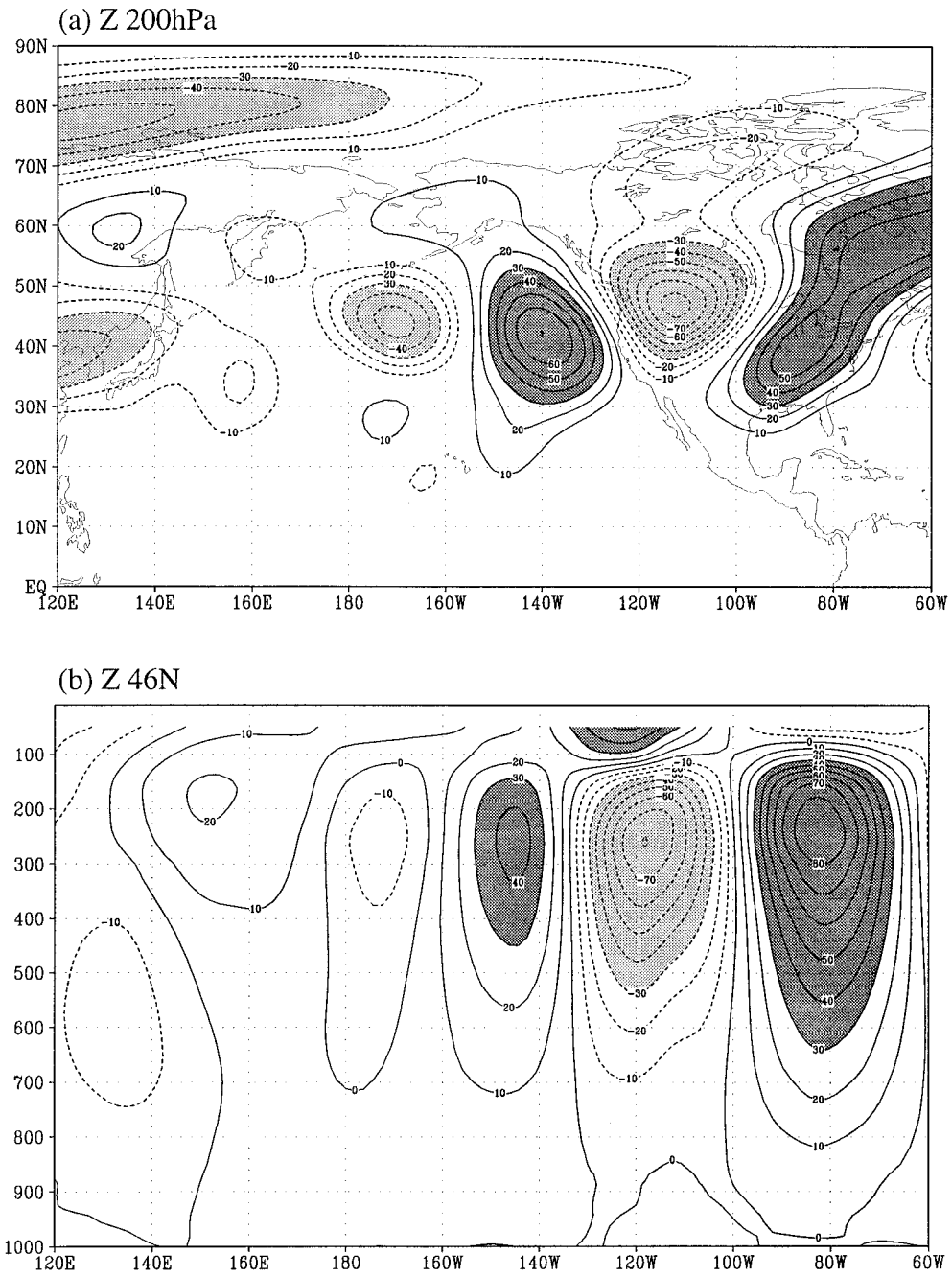

FIG. 3. Same as Fig. 2 except for JJA 1993 and the cross section (b) is at 46°N.

d. Anomalous transient forcings

The transient vorticity and thermal forcing is another important forcing mechanism for the maintenance of stationary wave anomalies. Part of the transient forcing is associated with anomalous storm track activities. One measure of the storm track anomalies is the bandpass filtered 850-hPa northward heat flux $\overline{v'T'}$, which is shown by shadings in Fig. 6. The bandpass filter is the same as that used by Blackmon (1976), which contains timescales from 2.5 to 6 days. The contours in Fig. 6 are the zonal wind anomalies, which closely relate to the transient anomalies. Enhanced northward heat flux over the central North Pacific in Fig. 6a is associated with an intensified Pacific jet. Over the land region in North America, the heat fluxes are also intensified even though the jet there is reduced. In 1993, the westerly jet over the Pacific is shifted farther south and reduced northward heat flux is found over most of East Asia and

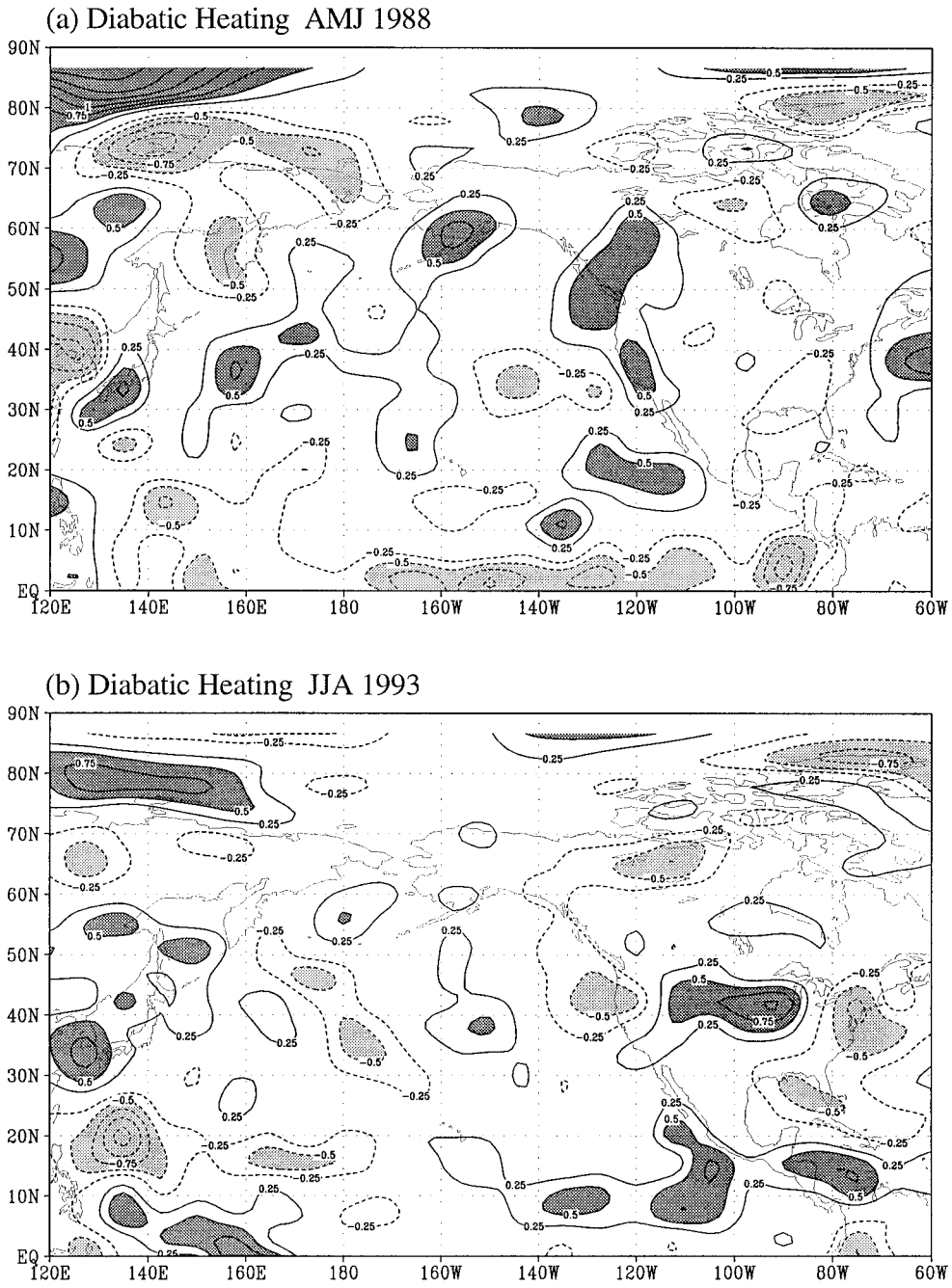

FIG. 4. Vertically integrated diabatic heating anomaly in (a) AMJ 1988 and (b) JJA 1993: CI = 0.25 K day^{-1}. Areas above 0.5 K day^{-1} are dark shaded and areas below -0.5 K day^{-1} are lightly shaded. Zero contours are omitted.

the North Pacific. Over North America, however, the westerly jet is intensified over the United States and weakened over Canada. These collocate with the enhanced northward heat flux.

The total transient forcing not only contains the high-frequency component, but the low-frequency (10–30 days) part as well. The relative importance between the high and low frequency variabilities can vary over time. For example, Mo et al. (1995) found that during 1993, the bandpass filtered transients were stronger in early summer, whereas the low-pass filtered transients were more dominant in middle summer. In the calculation below, the transients in both high- and low-frequency band will be considered together since the focus is the seasonal mean anomalies.

The transient forcings include both vorticity and heat

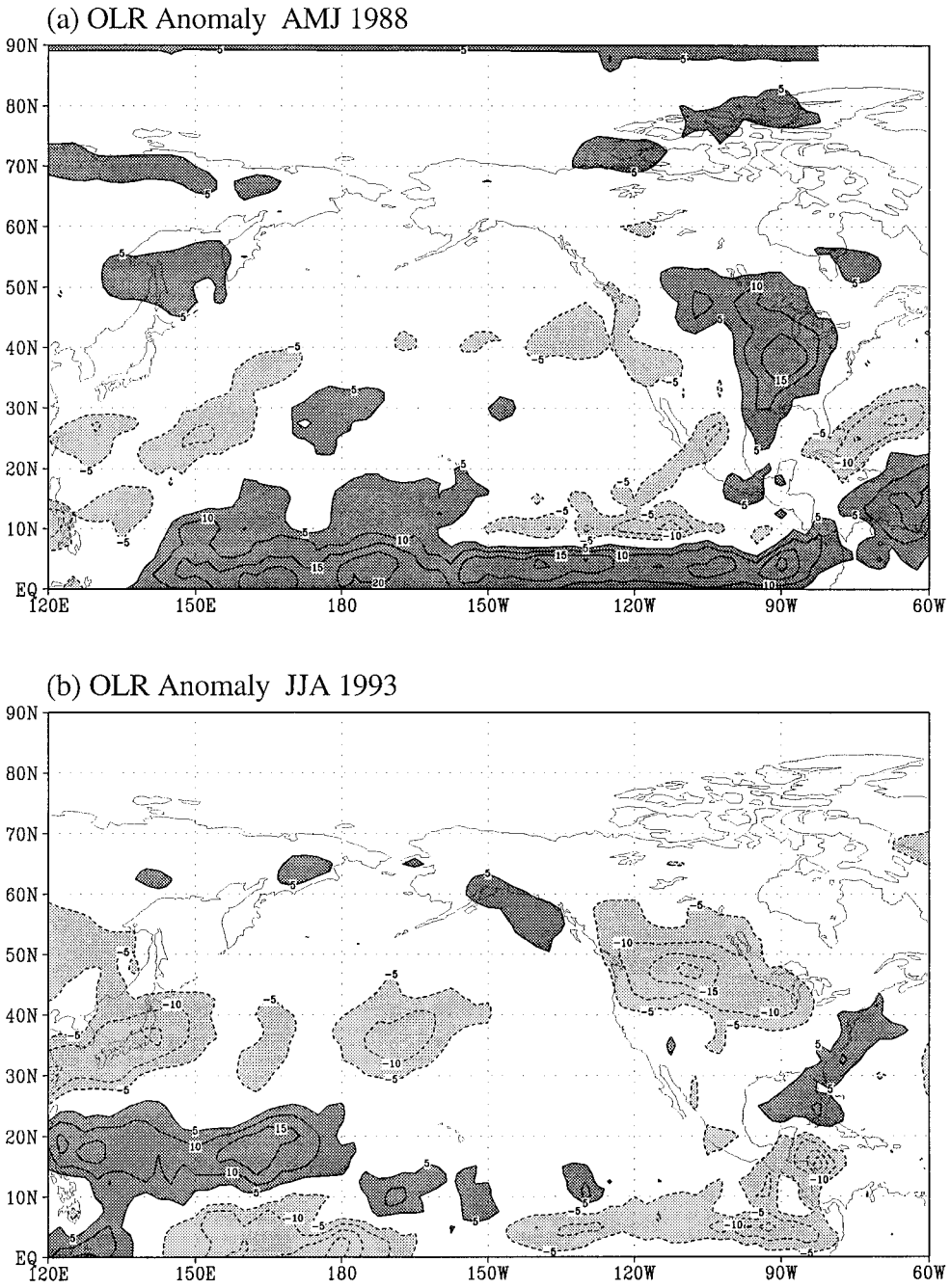

FIG. 5. Outgoing longwave radiation (OLR) anomaly in (a) AMJ 1988 and (b) JJA 1993: CI = 5 W m^{-2}. Areas above 5 W m^{-2} are dark shaded and areas below -5 W m^{-2} are lightly shaded. Zero contours are omitted.

flux convergences. The heat flux convergence is relatively small compared to the diabatic heating. The vertically integrated streamfunction tendency due to submonthly vorticity transients is shown in Fig. 7. The most dominant feature in 1988 (Fig. 7a) is the dipole structure over the United States, with an anticyclonic tendency over the western part and a cyclonic tendency over the eastern part. Both features correspond well with the height anomalies in Fig. 2a, indicating the possible effect of transient forcings on the seasonal mean flow. Farther upstream, there are cyclonic tendencies along the west coast of North America and anticyclonic tendencies over the central Pacific. In 1993, North America is dominated by the cyclonic tendency, in contrast to the anticyclonic tendency in 1988. The streamfunction tendency in 1993 agrees well with the corresponding height anomaly in Fig. 3a. This general agreement suggests that the transients have a positive feedback on the

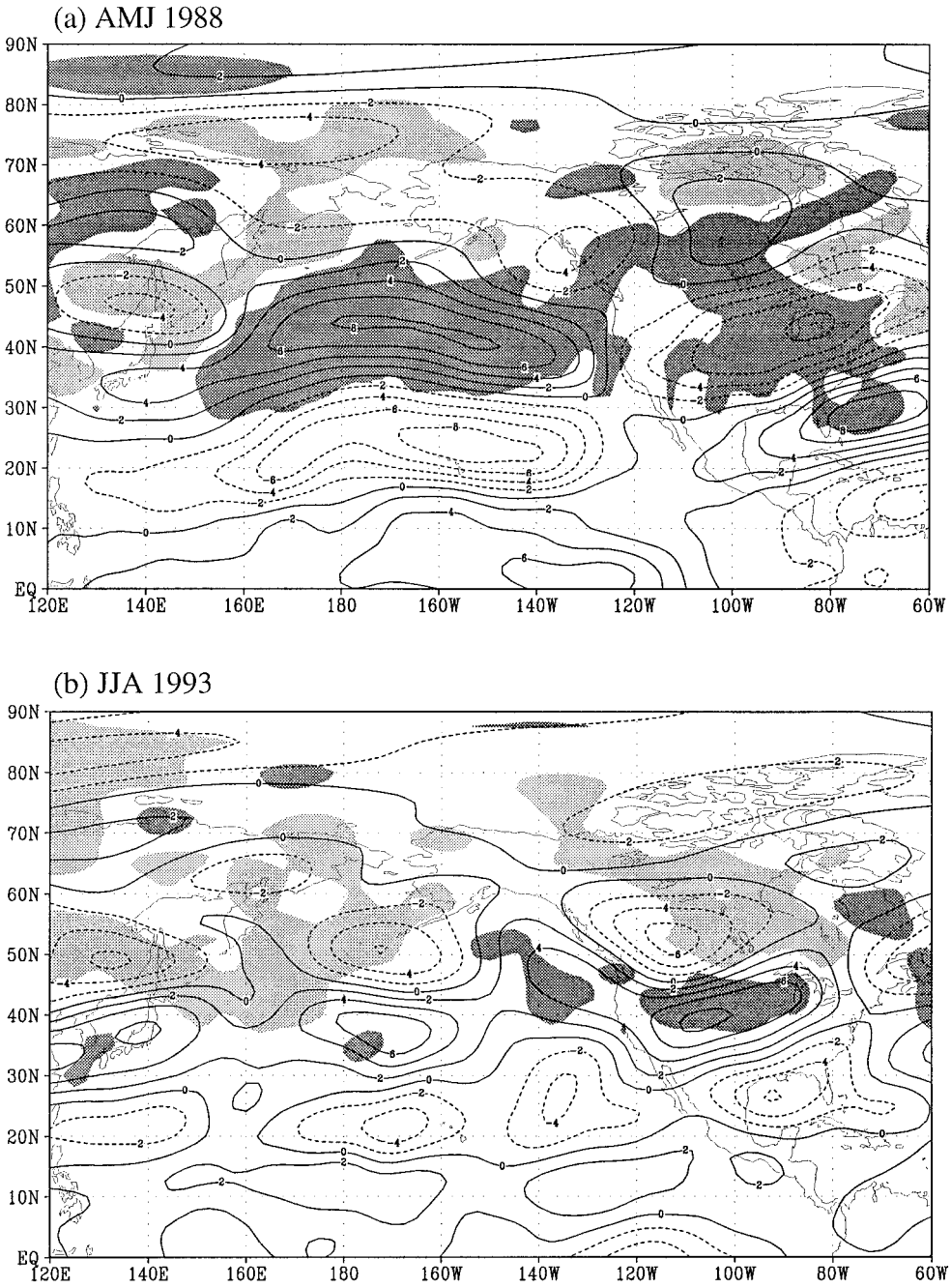

FIG. 6. Observed 850-hPa bandpass filtered $\overline{v'T'}$ anomaly (shading) and 200-hPa zonal wind anomaly (contour) in (a) AMJ 1988 and (b) JJA 1993. Dark-shaded areas are $\overline{v'T'} > 0.5$ K m s^{-1} and lightly shaded areas are $\overline{v'T'} < -0.5$ K m s^{-1}: CI = 2 m s^{-1} for zonal wind anomaly. Negative contours are dashed.

seasonal mean anomalies. This positive relation is valid for both the 1993 floods and the 1988 drought.

4. Linear model results

a. Response to total forcings

We first apply all the forcings to the stationary wave model and compare the response generated by the total forcing with the observed stationary wave anomalies. This provides a basis for further decomposing the response into those due to different components of the forcings. The model response of the 200-hPa Z is shown in Fig. 8 and Fig. 9 for AMJ 1988 and JJA 1993, respectively. They are to be compared with the corresponding observations shown in Figs. 2 and 3, respectively.

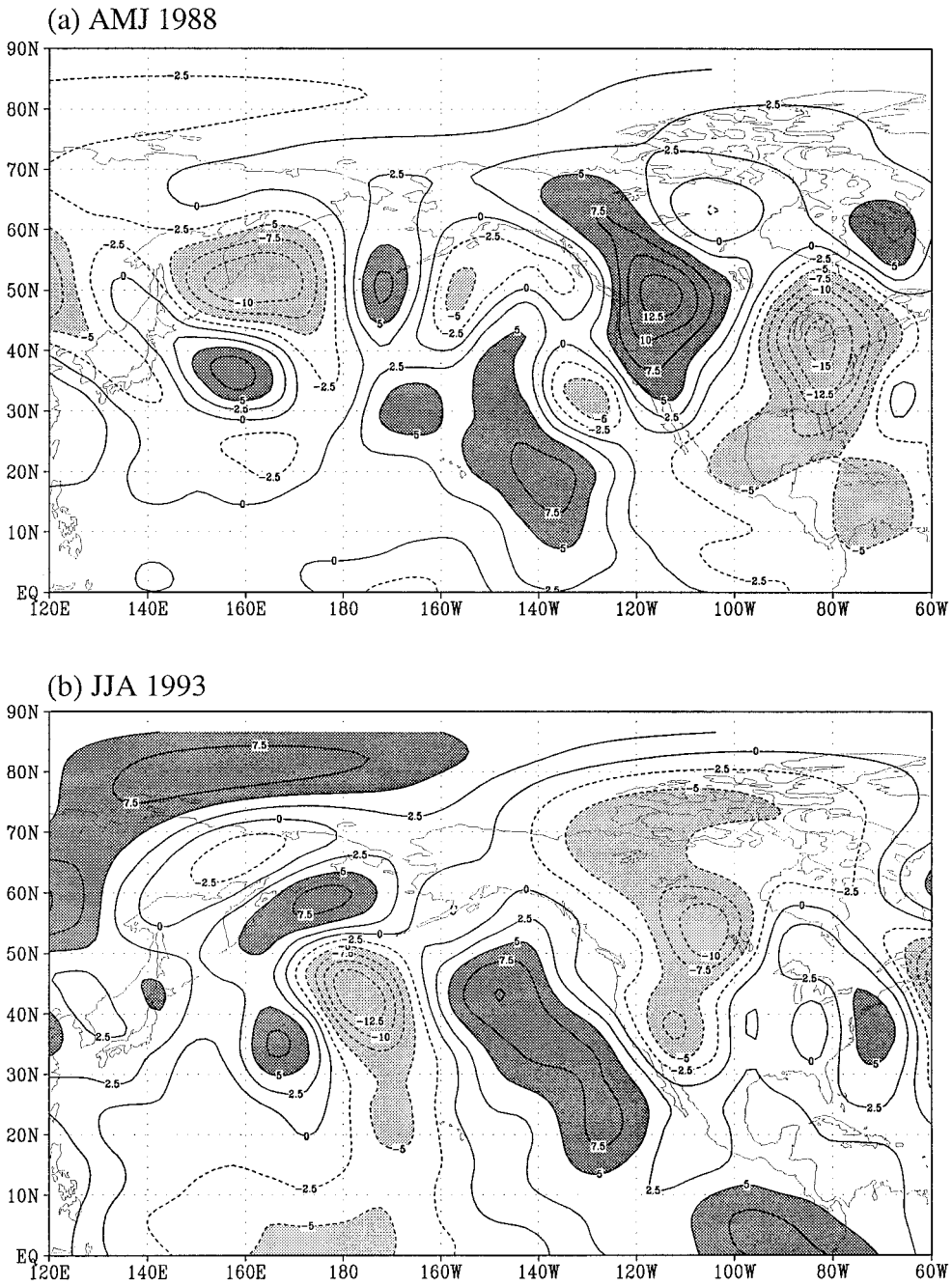

FIG. 7. Vertically integrated streamfunction tendency due to vorticity flux convergence anomaly in (a) AMJ 1988 and (b) JJA 1993: CI = 2.5 $m^2\ s^{-2}$. Areas above 5 $m^2\ s^{-2}$ are dark shaded and areas below -5 $m^2\ s^{-2}$ are lightly shaded.

In 1988, the model produced a similar wavelike anomaly pattern from the central Pacific to North America as in observations. Over North America, the model produced an anticyclonic anomaly with amplitude over 100 m, compared to an 80-m center in Fig. 2a. There is a slight westward shift in the center location over North America in the linear model. The vertical distribution of the model response (Fig. 8b) shows a similar equivalent barotropic structure as in observations (Fig. 2b). Since the vertical structure of Z is linked with the temperature through the hydrostatic balance, this agreement in vertical structure infers that the temperature structure is also well simulated (not shown).

To quantify how well the linear model reproduces the observed anomalies, we calculated the area-weighted pattern correlation and the root-mean-square (rms) am-

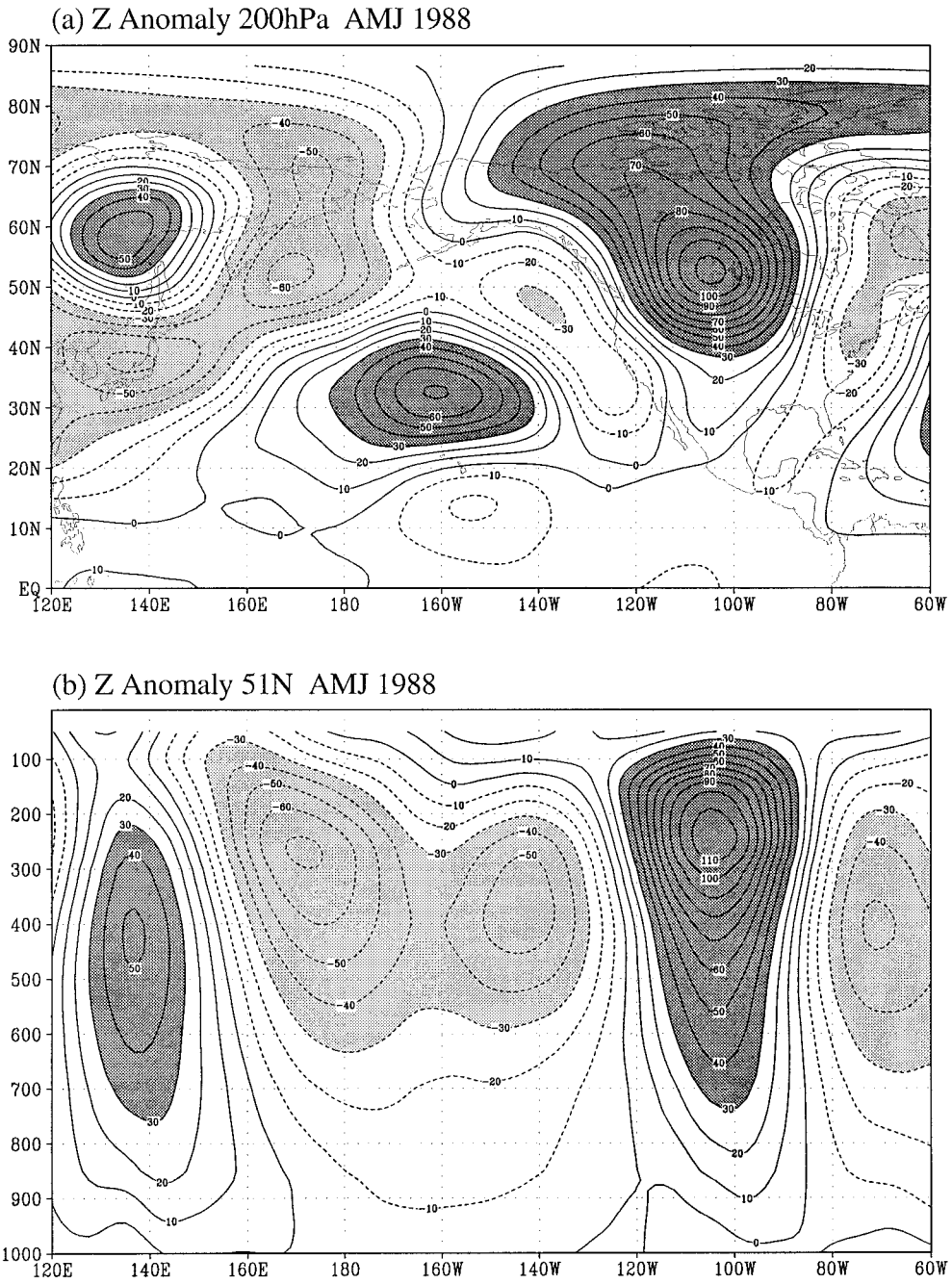

FIG. 8. Model-calculated zonally asymmetric Z anomaly in AMJ 1988. (a) Horizontal distribution at 200 hPa and (b) vertical–longitude cross section at 51°N: CI = 10 m. Areas above 30 m are dark shaded and areas below −30 m are lightly shaded.

plitude over the Pacific and North American domain (equator to 90°N, 120°E to 60°W). The results are shown in the first two rows of Table 1. The pattern correlation between observation and the linear model response to total forcing reaches 0.67 and the rms amplitude of the model response (29 m) is stronger than observations (25 m). The imperfect correlation between model response and observations is mainly contributed by discrepancies over East Asia and high latitudes. By removing the area north of 70°N, the correlation increases to 0.71 and the rms amplitude reduces to 26 m. The cause for the discrepancy can be many fold. Both the linear model formulation and the quality of the forcing data may contribute. The linear model has known resonant behaviors when linearized about the three-dimensional winter basic state (Branstator 1990; Ting and Sardeshmukh

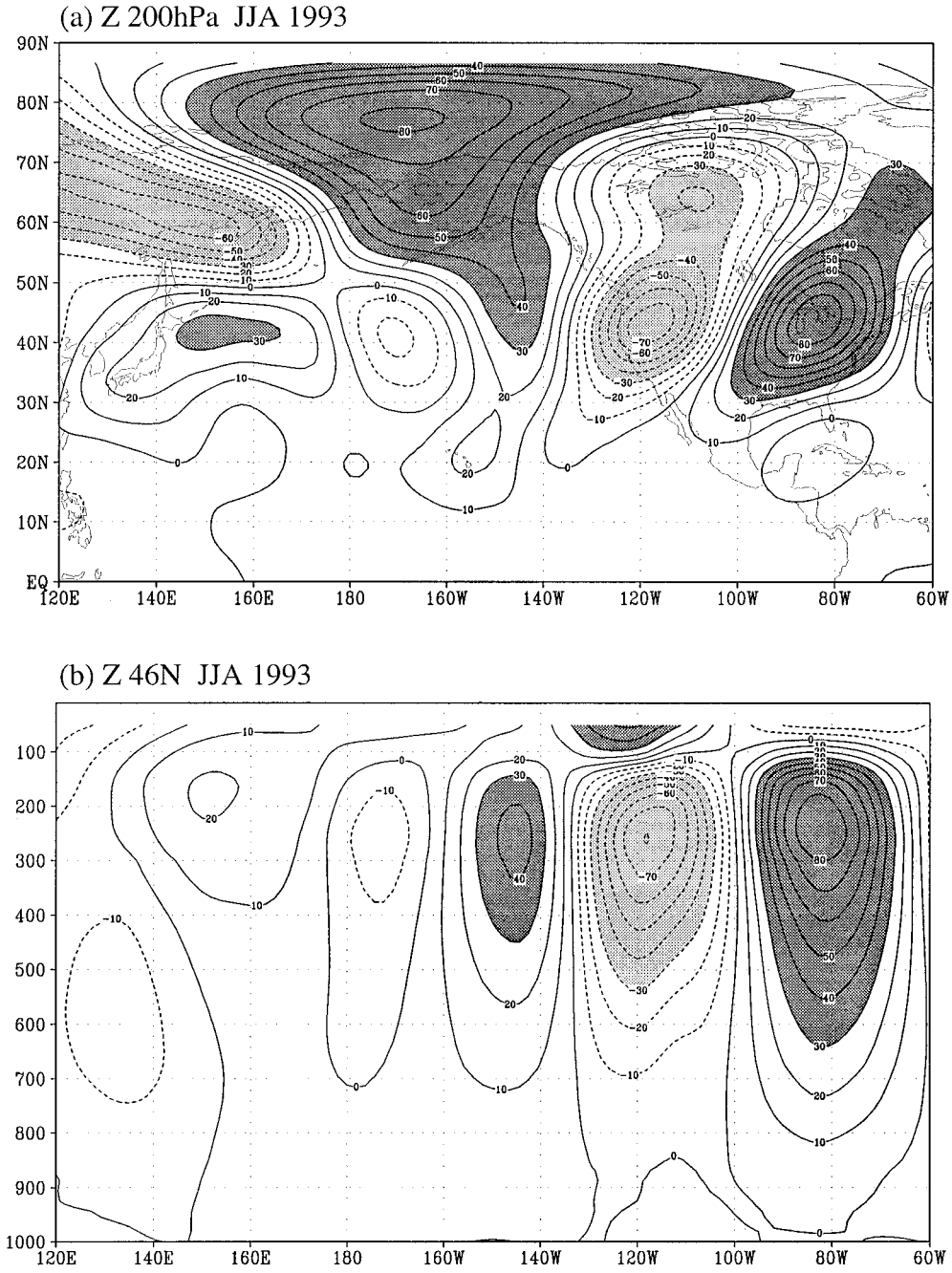

FIG. 9. Same as Fig. 8 except for JJA 1993 and the cross section (b) is at 46°N.

1993). Thus the linear model solution can be sensitive to the damping parameters chosen. There are great uncertainties to the precise choice of damping coefficients. The model resolution (R15) may also cause problems due to its inability to resolve the finescale features in the forcing data. The derived diabatic heating field is subject to many potential errors and relies heavily on the poorly observed vertical motion field. Given these uncertainties, the agreement between model results (Fig. 8a) and observations (Fig. 2) is rather remarkable.

For 1993, the model did reasonably well in reproducing the observed anomaly pattern over the North Pacific and North America. The significant low center over the northwestern United States is well simulated in both location and strength. The anticyclonic center over the U.S. East Coast agrees with observations in center location, but the amplitude is somewhat too strong. Over the North Pacific, however, the model-produced anomaly compares poorly with observations; in particular, the amplitude of the linear model response

TABLE 1. Area-weighted spatial pattern correlation and rms *Z* amplitude at 200 hPa in AMJ 1988 for the area 120°E–60°W, and equator to 90°N. The numbers in parentheses are for the area 120°E–60°W and 0°–70°N.

	Rms *Z* (m)	Correlation with observation	Correlation with model total
Observation	25.0 (25.0)	1.0	0.67 (0.71)
Model total	29.4 (26.1)	0.67 (0.71)	1.0
Diabatic heating	19.6 (19.1)	0.64 (0.67)	0.80 (0.77)
Transient vorticity flux	13.7 (13.5)	0.60 (0.59)	0.40 (0.45)
Transient heat flux	14.3 (14.2)	−0.16 (−0.19)	0.16 (0.20)

TABLE 2. Area-weighted spatial pattern correlation and rms *Z* amplitude at 200 hPa in JJA 1993 for the area 120°E–60°W and 0°–90°N. The numbers in parentheses are for the area 120°E–60°W and 0°–70°N.

	Rms *Z* (m)	Correlation with observation	Correlation with model total
Observation	18.5 (18.2)	1.0	0.47 (0.58)
Model total	24.5 (23.3)	0.47 (0.58)	1.0
Diabatic heating	17.2 (16.6)	0.27 (0.30)	0.83 (0.83)
Transient vorticity flux	11.8 (11.9)	0.49 (0.55)	0.68 (0.68)
Transient heat flux	6.1 (6.0)	0.04 (0.11)	0.36 (0.30)

is much too weak. The largest discrepancy between the model and the observation exists over northern high latitudes, where the linear model produces a spurious positive center, which does not have any counterpart in observations. Comparing Fig. 9b with Fig. 3b, one can see that the vertical structure is again well simulated, with equivalent barotropic structure throughout the main centers of anomalies.

The spatial pattern correlation between observed anomalies and model responses at 200 hPa (Table 2) is only 0.47, much lower than the 1988 counterpart. By removing the area north of 70°N, the correlation increases to 0.58. The large discrepancies over the northern high latitudes contributed significantly toward the low spatial correlation. Even though the model response is weaker than observations over the Pacific, the rms amplitude in the model (24.5 m) is much higher than in observations (18.5 m). As will be shown later, the lower correlation is mainly due to the diabatic heating forcing. Again, the uncertainties in the derived diabatic heating may be important.

b. Contributions from different forcings

The forcings used in the previous section include the vorticity flux convergences, heat flux convergences, diabatic heating, and nonlinear forcing. The linear model responses to the four forcings in isolation for AMJ 1988 are shown in Fig. 10. Significant amplitudes are found for responses to diabatic heating (Fig. 10a), transient vorticity (Fig. 10b), and heat (Fig. 10c) flux forcings. Over the United States, for example, the dominant anticyclone is forced by the integrated effect of transient vorticity and thermal forcings. Over the central North Pacific and Canada, on the other hand, the effect of diabatic heating apparently dominates. The stationary nonlinear forcing produced negligible response in most areas.

It is interesting to note that the well-defined wave train over the Pacific and North American domain, shown as the response to total forcing in Fig. 8a, is a result of the combination of different forcing components, rather than a single forcing mechanism. The effect of the diabatic heating tends to produce the anticyclonic centers over the central Pacific and Canada, whereas the transient vorticity forcing is responsible for the low centers over the Gulf of Alaska and the U.S. Southeast, as well as the anticyclone over the western United States. It is somewhat misleading to view the wave train as the great circle wave propagation due to a single source. The spatial pattern correlation between the linear model response to each individual forcing and observations as well as model response to total forcing are included in Table 1. Although the response to diabatic heating correlates highly with the model response to total forcing (0.80), it is not as highly correlated with observations (0.64). This indicates that part of the deficiencies of the model response to total forcing (Fig. 8a) may be due to errors in diabatic heating. Indeed by comparing Fig. 10a with Fig. 8a, one finds that most of the unrealistic features in Fig. 8a over East Asia and northern high latitudes are due to the effect of diabatic heating. By removing the area north of 70°N, the correlation between the effect of heating and observations increases to 0.67. The correlation between response to diabatic heating and observations is comparable to the correlation between response to total forcing and observations, and stronger than the correlation of any other forcing mechanisms. The rms amplitude due to heating (~19 m) is the strongest among the four forcing mechanisms. Apparently AMJ 1988 atmospheric anomalies are dominated by the effect of diabatic heating. The effect of transient vorticity forcing, although of smaller amplitude, also correlates significantly with the observed anomalies (0.6). The effect of transient thermal forcing, though of comparable rms amplitude to the effect of vorticity forcing, correlates poorly with both observations and model response to total forcing.

The same decomposition for 1993 is shown in Fig. 11. Over North America, the contribution to total anomalies due to diabatic heating is slightly weaker than those due to the vorticity forcing, although of similar spatial pattern. The contribution due to transient heat flux and the nonlinearity is much weaker than the other two forcings. Over the North Pacific, there are partial cancellations due to different forcings and the relative contribution due to each forcing is more difficult to assess. The spatial pattern correlations (Table 2) of the effect

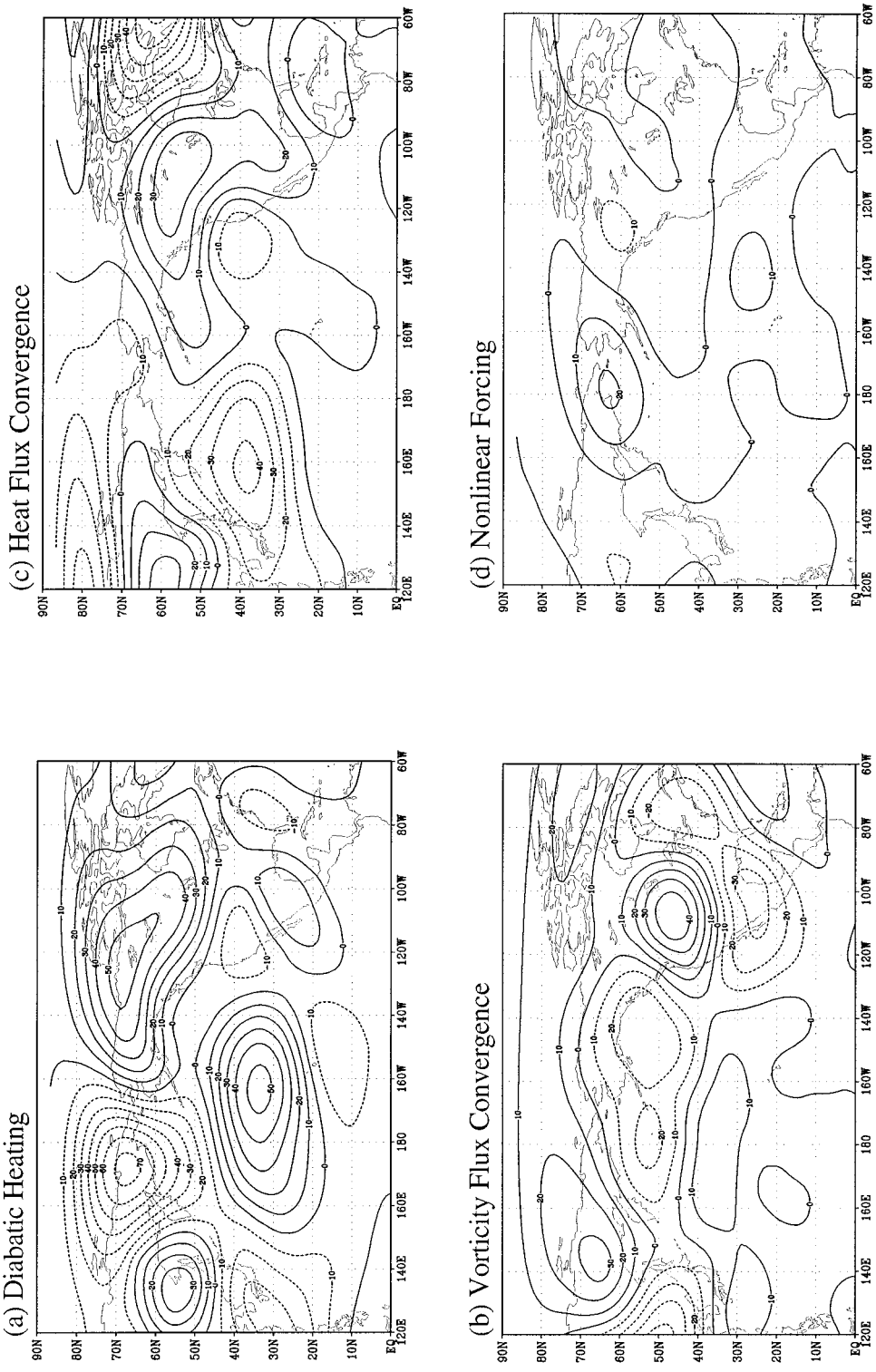

FIG. 10. Model-calculated zonally asymmetric 200-hPa Z anomaly at in AMJ 1988 due to (a) diabatic heating, (b) vorticity transients, (c) thermal transients, and (d) stationary nonlinearity: CI = 10 m and negative contours are dashed.

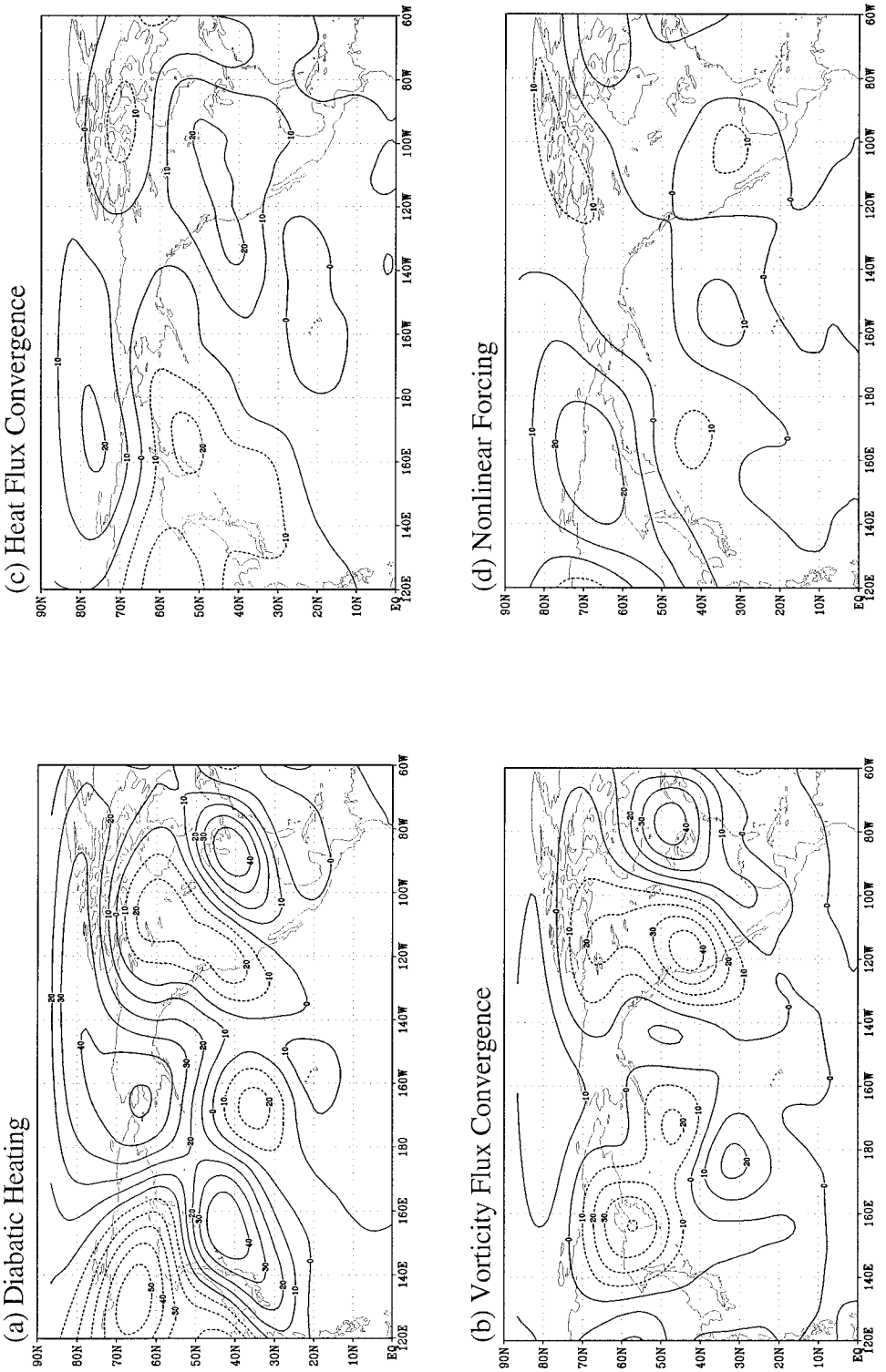

FIG. 11. Same as Fig. 10 except for JJA 1993.

of different forcing mechanisms with model response to total forcing are generally quite high, whereas those with observations relatively low. The highest correlation with observed anomalies is found for the effect of vorticity transient forcing (0.49). The effect of diabatic heating correlates very highly with total model response (0.83), but poorly with observations (0.27). This indicates that the relatively small pattern correlation between total model response and observations (0.47) in 1993 is due mainly to the contribution of diabatic heating. When removing the area north of 70°N, the correlation increases significantly between response to vorticity flux forcing and observations (0.55), and only slightly between response to diabatic heating and observations (0.30). Based on the pattern correlations, it is reasonable to conclude that the effect of vorticity transients is the most dominant forcing mechanism for the 1993 flood circulation. The importance of the transient vorticity forcing in maintaining the 1993 summer circulation anomalies is in agreement with Mo et al. (1995), who suggested that the anomaly pattern over the United States in the summer of 1993 is a result of a strengthened westerly jet induced by strong transient eddy momentum fluxes.

c. Regional diabatic heating contributions

The importance of the diabatic heating contribution to the geopotential height anomalies over most of the regions in both seasons warrants further examination of the areas that contribute the most to the anomalous circulation. An important issue for the 1988 drought is to determine whether the stationary wave anomalies produced by the diabatic heating are from a remote or local source. As shown in Fig. 4a, the anomalous diabatic heating field in 1988 has several centers around the Pacific and over North America. To determine in which regions the diabatic heating contributes most to the total anomaly, we consider the following six regions: the subtropical eastern Pacific (A), the equatorial Pacific (B), the western Pacific (C), the eastern central Pacific (D), and the west coast of North America (E) and the United States (F). For each region, only the diabatic heating inside the region is used as the forcing in the linear model to produce the stationary wave response. The model response to the diabatic heating in these six regions is shown in Fig. 12 (the contour interval has been reduced by half compared to previous figures). The shading indicates the region of nonzero diabatic heating. When determining the heating boundaries, we took into account the actual heating distribution in Fig. 4a so that major heating centers are not separated into parts.

The eastern subtropical Pacific (Region A) heating anomaly is associated with the northward shift of the ITCZ in 1988. Trenberth and Branstator (1992) argued that this heating anomaly was mainly responsible for the generation of the observed wave train (Fig. 2a). Our model result (Fig. 12a) shows that the effect of this heating anomaly is rather limited. It generates height anomalies of about 5–15 m over the United States and does not exhibit a strong wavelike signature. Figure 12b demonstrates that the cooling over the equatorial Pacific (Region B) produces negligible response over both the North Pacific and North America. Thus, the anomalous heating and cooling associated with La Niña SST anomalies over the equatorial Pacific is not a major factor for the AMJ 1988 stationary wave anomalies. The response to the western Pacific (Region C) heating is very strong over the whole North Pacific, and extends to Canada (Fig. 12c). The large amplitude response contributes strongly toward the northward shifted and intensified Pacific jet stream. The importance of the western Pacific heating to the evolution of the 1988 drought is emphasized in a recent study by Chen and Newman (1998). Our result in Fig. 12c is in agreement with Chen and Newman (1998) on the possible triggering of the 1988 U.S. drought. The intensified and northward shifted Pacific storm track may contribute to both the anomalous transient vorticity forcing and the diabatic heating over the eastern North Pacific region. The negative heating anomaly over the eastern central Pacific (Region D) generated a strong cyclonic anomaly downstream, centered over the California coast and extends to a large part of the United States (Fig. 12d). It also contributes to the high anomaly over Canada. The negative height anomaly over the United States partly compensates the largest positive height anomaly generated by the heating over the west coast of North America (Region E, Fig. 12e). Both the cooling in Region D and the heating in Region E can be consequences of the anomalous storm activity due to the northward shifted storm track in AMJ 1988. The combined effect of the heating in Regions C, D, and E dominates the anticyclonic responses over the Pacific and Canada in Fig. 10a. The cooling associated with the drought in AMJ 1988 (Region F) produced a low center to the southeast and a weak high anomaly over the northwest of the United States. As suggested by the OLR, the cooling over the United States is underestimated in the residual heating calculation. Thus the weaker cyclonic anomaly over the southeast United States in the linear model simulation (Fig. 8a) compared to observations (Fig. 2a) can be partly due to this underestimation. The result in Fig. 12f suggests a positive feedback between the drought-induced cooling and the circulation anomalies during the 1988 drought.

Figure 12 strongly suggests that the remote diabatic forcing from the Tropics is not an important contributor toward the drought circulation in 1988. The western Pacific heating, and the related storm track heating and cooling anomalies over the eastern Pacific and the west coast of North America, on the other hand, dominates the total atmospheric response to global heating. The heating-induced circulation, combined with the transient vorticity and heat flux convergences, maintains the AMJ 1988 circulation anomalies.

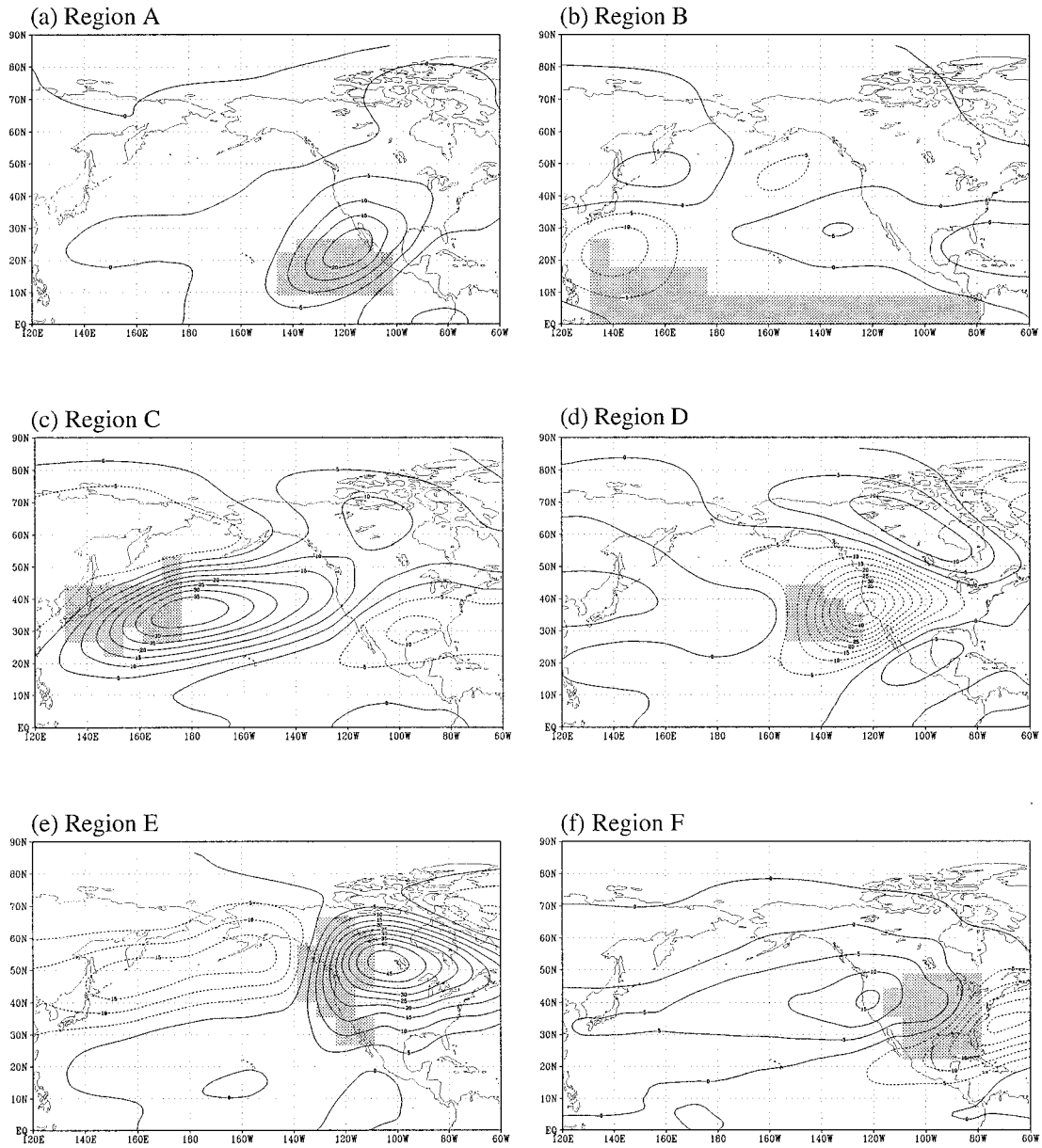

FIG. 12. Model 200-hPa *Z* response to regional diabatic heating in AMJ 1988: CI = 5 m and negative contours are dashed. Shaded areas are regions where the diabatic heating is used.

We have also performed similar experiments with the 1993 diabatic heating. The results (not shown) indicate that the cooling center over the U.S. West Coast in Fig. 4b produces a low center over central North America. It is largely compensated by the effect of the heating over the central United States. The latter also contributes to the high anomaly over the eastern United States in Fig. 11a. Thus, diabatic forcing in 1993 is dominated by those related to the flooding itself. Similar to 1988, the anomaly produced by diabatic heating is mainly from a local midlatitude source. The effect of the tropical diabatic forcing is negligible.

5. Green's function experiments

Due to uncertainties in the derived forcing fields, especially the diabatic heating fields, it is important to examine the extent to which conclusions drawn from the linear model budget analysis in section 4 are valid. We took the Green's function approach, which can address this concern. Given the observed circulation anomalies in Figs. 2 and 3, the Green's function calculation determines the regions of forcing that will contribute the most toward the anomalous circulation anomalies at a particular location.

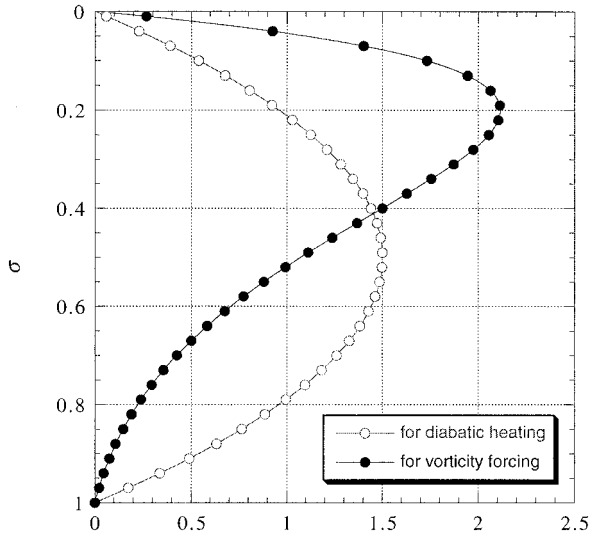

FIG. 13. Specified vertical distributions of diabatic heating and vorticity forcing in Green's function experiments.

We consider both the diabatic heating and vorticity transient forcing in this section. As discussed in section 2, the vertical structure of the Green's function forcing is prescribed. For the diabatic heating, we use a vertical profile with maximum at $\sigma = 0.5$ and vertically integrated intensity of 1 K day^{-1}. For the vorticity forcing, we use a vertical profile with maximum at $\sigma = 0.2$ and vertically integrated intensity of 5×10^{-11} s^{-2}. These vertical profiles are shown in Fig. 13. The intensity and the vertical distribution are chosen to be representative of the typical forcing.

The selection of the reference points (λ^*, ϕ^*) is based on the centers of the observed 200-hPa Z anomalies shown in Figs. 2a and 3a. For 1988, we choose three points corresponding to the centers of the high over the central Pacific, the high over North America, and the low over the U.S. Southeast, respectively. For these three points, we use AMJ climate as basic state for the Green's function calculation. For 1993, we choose three points corresponding to the centers of the high over the eastern North Pacific, the low over North America, and the high over the eastern United States, respectively. We use JJA climate as the basic state for these three points. Notice that these points are chosen because they are most relevant for the stationary wave anomaly patterns during the 1988 drought and 1993 floods. The Green's function, however, does not depend on the actual anomalies in 1988 or 1993. It only depends on the basic state and the location of the reference point.

a. Green's function for diabatic heating

The Green's functions for these six reference points for diabatic heating are shown in Fig. 14. In all six cases, the Green's functions do not have large amplitude over the equatorial Pacific, consistent with the calculation in section 4. The region where the diabatic heating has the largest impact (maximum centers) on the stationary wave anomalies at the reference point is either to the west or to the southwest of the reference point. Therefore it is the local or upstream diabatic heating that is most responsible for the midlatitude stationary wave anomalies over the North Pacific and North America.

Even though Figs. 14a–c and Figs. 14d–e were calculated based on different basic states, the AMJ and JJA climate are similar enough that their Green's functions do not differ very much. Over the Pacific in both Fig. 14a and 14d, the Green's function is longitudinally elongated with a maximum a few degrees to the west of the reference point. Therefore a heating that is located several degrees to the west is most effective in generating an anomaly downstream. Figures 14b and 14e are also similar with a wave-train-like structure to the southwest of the reference point. For the reference points over the United States (Fig. 14c and 14f), the Green's functions are more compact and cover most of the U.S. continent. We have also calculated the Green's functions at many other reference points over the United States and found that, in general, the most effective forcing region is over the western part of the United States, and southwest of the reference points. This distribution may be explained by the structure of the basic flow shown in Figs. 1b and 1d. The U.S. West Coast is in the exit region of the Pacific jet. The westerly flow along the West Coast is relatively weak. Held and Ting (1990) argued that the response to a midlatitude heat source is inversely proportional to the strength of the zonal flow at the heated level. The weaker the zonal flow, the larger the response. Thus, a heat source located over the U.S. West Coast would produce a larger response downstream over the United States than a similar source located farther inland. The negative centers to the southwest of the positive center in Fig. 14b and 14e indicate that cooling in this region can also contribute to the positive 200-hPa Z anomaly over North America.

By combining the Green's functions with the actual diabatic heating distribution in 1988 and 1993, we can get a better understanding of the cause of the stationary wave anomalies in these two years. In 1988, the diabatic heating anomaly over the west coast of North America (Fig. 4a) is within the positive Green's function region in Fig. 14b and close to the maximum center of the Green's function. Therefore it contributes most to the high anomaly over Canada (Fig. 10a). The cooling areas over the eastern central Pacific (Fig. 4a) also contribute to the high anomaly over Canada since the Green's function there is negative (Fig. 14b). The strong anticyclonic anomaly over the central Pacific (Fig. 10a) is induced by the diabatic heating over the western Pacific (Fig. 4a) according to the Green's function in Fig. 14a. In 1993, the cooling over the U.S. West Coast (Fig. 4b) contributes most to the low anomaly over the western United States since the cooling region falls within the positive Green's function in Fig. 14e. It is largely compensated by the heating over the United States

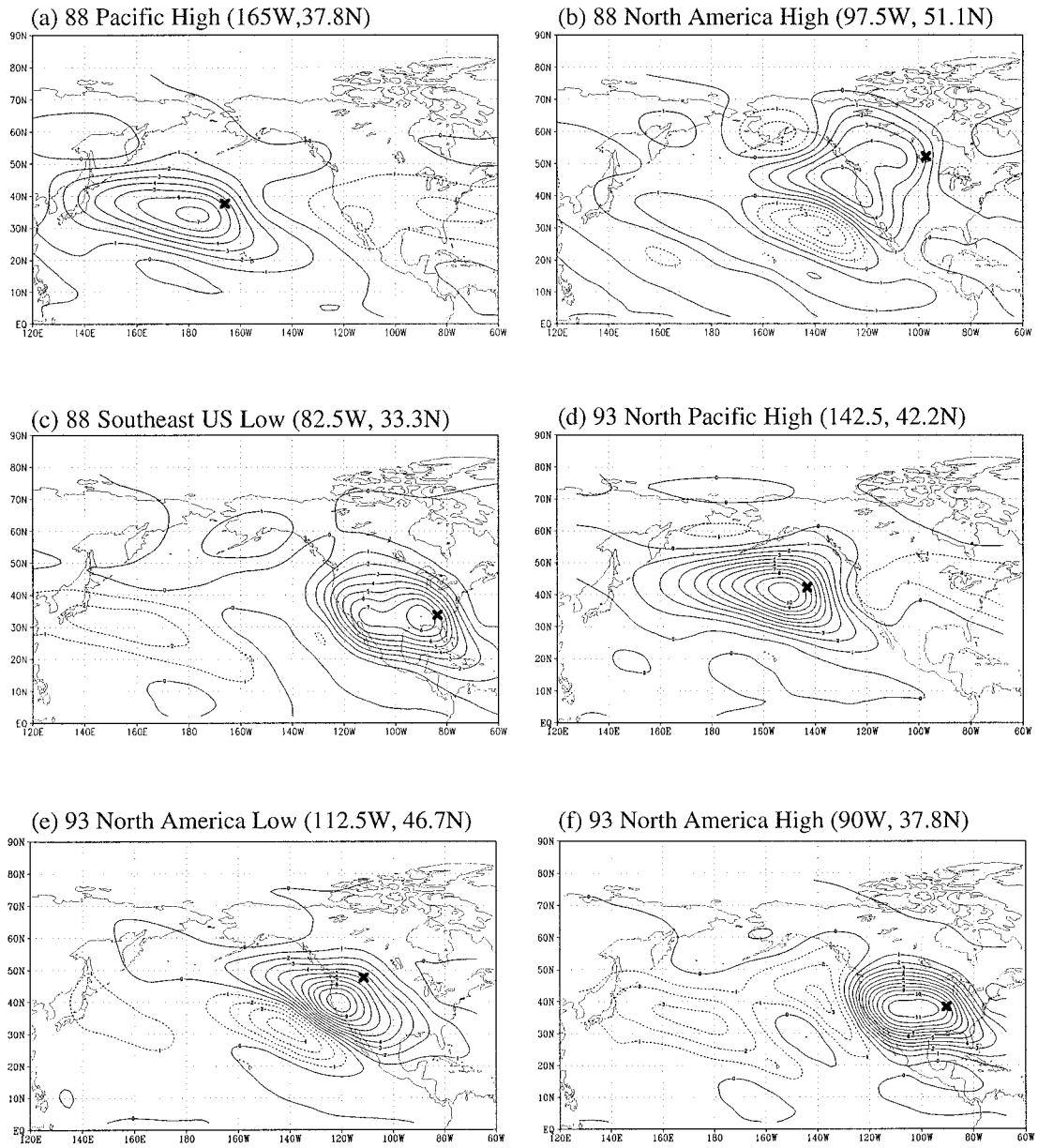

FIG. 14. Green's function of diabatic heating for 200-hPa Z at six points indicated by a cross: CI = 1 m and negative contours are dashed.

since the Green's function is of the same sign in both the cooling and heating regions (Fig. 14e). Based on the Green's function results (Fig. 14e), the cooling over the U.S. West Coast is at the optimal location for generating the North American low. The possible influence of this cooling on the strength and severity of the 1993 floods is worthy of further investigation.

b. Green's function for transient vorticity flux convergence

The Green's functions for vorticity forcing for the same six points are shown in Fig. 15. The response to vorticity forcing is very different from that to diabatic heating. For all six points, there is a negative center close to the reference point, indicating that a local vorticity forcing always maintains and intensifies the stationary wave anomalies. The alternating maximum/minimum centers in other regions suggest that remote vorticity forcing can contribute significantly to the local response. By comparing the vorticity forcing in Fig. 7 and the Green's functions in Fig. 15, one can find the major contributors to the stationary anomalies. For example, the low anomaly to the southeast of the United States (Fig. 10b) is related to the local vorticity forcing (cf. Fig. 15c and Fig. 7a). In 1993, the anticyclonic

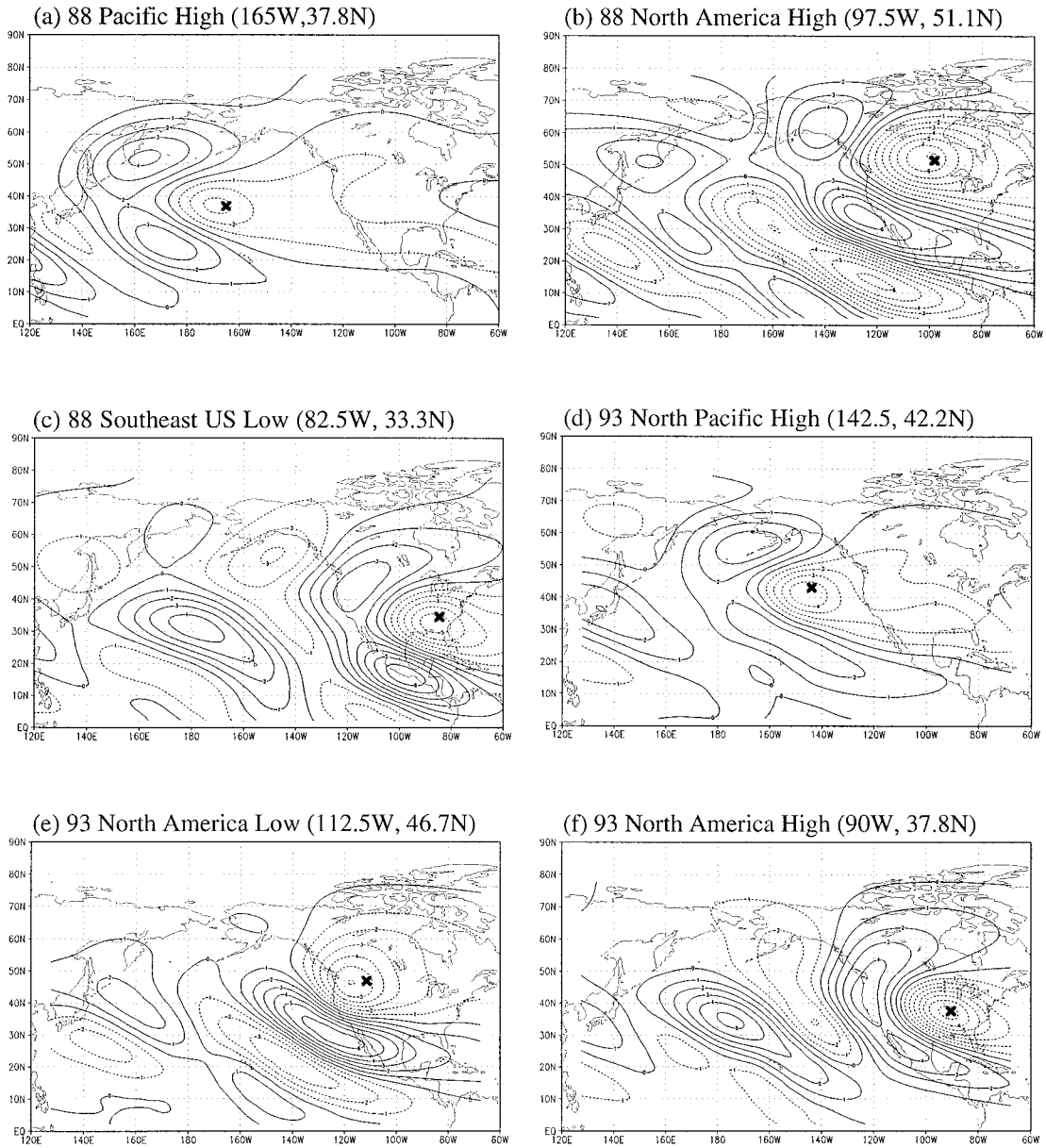

FIG. 15. As in Fig. 14 but for vorticity forcing.

forcing over the eastern Pacific (Fig. 7b) contributes to the low over the western part of North America (Fig. 11b) since the forcing area coincides with the positive Green's function in Fig. 15e.

6. Summary and discussion

We have investigated the stationary wave anomalies in spring of 1988 and summer of 1993 based on linear dynamics. The recently available NCEP Reanalysis data has proved to be useful in providing reasonably realistic forcing fields, which lead to reasonable simulations of the stationary wave anomalies in these two seasons. The linear baroclinic model linearized about the zonally varying seasonal mean climatology has proved to be a valid tool for simulating the spring and summer anomalous stationary waves. The linear model simulation compares better with observations for AMJ 1988 than JJA 1993, for reasons not completely understood. Additional calculation shows that the latter conclusion is not a result of the differences in AMJ and JJA basic states.

By examining the response to the transient forcing and diabatic heating separately, we have shown that the diabatic heating and transient forcing are both important to the circulation anomalies in 1988; whereas the transient vorticity forcing is the most dominant forcing mechanism to the circulation anomaly in 1993. This

result is in agreement with other studies indicating that the transient eddy forcing is important for the 1993 anomaly pattern (Mo et al. 1995). We further examined the diabatic heating effect in 1988 separately in six regions: the subtropical eastern Pacific, equatorial Pacific, western Pacific, eastern central Pacific, west coast of North America, and the United States, in order to identify which region of the diabatic heating is responsible for the North American anomaly in 1988. The results indicate that the heating over the equatorial Pacific and the eastern Pacific has negligible contribution to the North American anomaly. The diabatic heating along the west coast of North America contributes most to the anticyclonic anomaly over North America in 1988. In 1993, the anomaly produced by North Pacific cooling is compensated by local heating over North America, resulting in a weak response to the total diabatic heating. Therefore, even though the response to the total diabatic heating is weak in 1993, the importance of the diabatic heating cannot be discounted.

To determine which region is most favorable for the excitation of the observed stationary wave anomalies, we calculated the Green's function for diabatic heating and vorticity forcing. The Green's function for diabatic heating confirms our results from regional heating experiments that the stationary wave anomaly is largely the response to a local midlatitude heat source; the equatorial Pacific has no significant influence on the observed stationary wave anomalies. Particularly, in the spring of 1988, the anomalous high over North America is mainly associated with the diabatic heating along the west coast of North America. The Green's function for the vorticity forcing shows a wave train pattern generally extending westward or southwestward of the reference point. Based on the actual vorticity forcing distribution, the vorticity-forcing-induced anomaly over North America in 1988 and 1993 is largely due to local vorticity forcing, rather than remote forcing.

The possible role of the western Pacific heating in initiating the 1988 drought circulation is also noted. Chen and Newman (1998) argued in their recent study that the time evolution of the 10-day mean streamfunction anomalies during May and June of 1988 indicates the important triggering mechanism of the western Pacific divergence. Our results here are consistent with their findings. The western North Pacific heating is almost entirely responsible for the anticyclonic circulation over the North Pacific in 1988. This anticyclonic center results in a significant northward shift and intensification of the Pacific jet, which may in turn cause the eastern Pacific heating and cooling anomalies, as well as the anomalous transient forcing over the North Pacific and North America. We note the important role played by the transient vorticity forcing and the possible role of the cooling over the west coast of the United States. The cause for these anomalous forcings is not apparent from our analysis, however.

The linear stationary wave model cannot be used to determine the ultimate cause for the drought/flood circulation. The linear model diagnostics help to understand the relative importance of the different dynamical forcing mechanisms. Many important processes, such as the soil moisture feedback and atmospheric moisture transport, cannot be taken into account in such a dynamical model. The linear model may suggest the key dynamical forcings for the drought/flood circulation, but the origin of such a forcing cannot be determined by the linear model. A more complete general circulation modeling experiment is necessary to fully understand the relative importance of the SST forcing, the soil moisture feedback, and the internal atmospheric processes in contributing to the drought and flood circulations. This study, however, strongly suggests that linear diagnostic models such as the one used in this study can be very useful in elucidating the effect of the various forcing mechanisms operating in the GCM as well as in the real atmosphere.

Acknowledgments. Support for this study is provided by NSF CAREER Award ATM9506368 and NOAA Grant NA56GP0150. The NCEP/NCAR Reanalysis data used in this study is distributed by the Climate Diagnostic Center in Boulder, Colorado. We would like to thank Prof. Walter Robinson and an anonymous reviewer for useful suggestions to an earlier version of the paper.

REFERENCES

Blackmon, M. L., 1976: A climatological spectral study of the 500 mb geopotential height of the Northern Hemisphere. *J. Atmos. Sci.,* **33,** 1607–1623.

Branstator, G., 1985: Analysis of general circulation model sea surface temperature anomaly simulations using a linear model. Part I: Forced solutions. *J. Atmos. Sci.,* **42,** 2225–2241.

——, 1990: Low-frequency patterns induced by stationary waves. *J. Atmos. Sci.,* **47,** 629–648.

——, 1992: The maintenance of low-frequency atmospheric anomalies. *J. Atmos. Sci.,* **49,** 1924–1945.

Chen, P., and M. Newman, 1998: Rossby wave propagation and the rapid development of upper-level anomalous anticyclones during the 1988 U.S. drought. *J. Climate,* in press.

Held, I. M., and M. Ting, 1990: Orographic versus thermal forcing of stationary waves: The importance of the mean low-level wind. *J. Atmos. Sci.,* **47,** 495–500.

Hoerling, M. P., M. Ting, and A. Kumar, 1995: Zonal flow-stationary wave relationship during El Niño: Implications for seasonal forecasting. *J. Climate,* **8,** 1838–1852.

Kalnay, E., M. Kanamitsu, R. Kistler, W. Collins, D. Deaven, L. Gandin, M. Iredell, S. Saha, G. H. White, J. Woollen, Y. Zhu, M. Chelliah, W. Ebisuzaki, R. W. Higgins, J. Janowiak, K. C. Mo, C. Ropelewski, J. Wang, A. Leetmaa, R. Reynolds, R. Jenne and D. Joseph, 1996: The NCEP/NCAR 40-Year Reanalysis Project. *Bull. Amer. Meteor. Soc.,* **77,** 437–471.

Kunkel, K. E., S. A. Changnon, and J. R. Angel, 1994: Climate aspects of the 1993 upper Mississippi River basin flood. *Bull. Amer. Meteor. Soc.,* **75,** 811–822.

Mo, K. C., J. Nogues-Paegle, and J. Paegle, 1995: Physical mechanisms of the 1993 summer floods. *J. Atmos. Sci.,* **52,** 879–895.

NOAA, 1988: *Climate Diagnostics Bulletin.* No. 88/4, 88/5, 88/6.

NOAA, 1993: *Climate Diagnostics Bulletin.* No. 93/6, 93/7, 93/8.

Ting, M., 1994: Maintenance of northern summer stationary waves in a GCM. *J. Atmos. Sci.*, **51,** 3286–3308.

——, and I. M. Held, 1990: The stationary wave response to a tropical SST anomaly in an idealized GCM. *J. Atmos. Sci.*, **47,** 2546–2566.

——, and P. Sardeshmukh, 1993: Factors determining the extratropical response to equatorial diabatic heating anomalies. *J. Atmos. Sci.*, **50,** 907–918.

——, and H. Wang, 1997: Summertime United States precipitation variability and its relation to Pacific sea surface temperature. *J. Climate*, **10,** 1853–1873.

——, T. Xu, and M. P. Hoerling, 1996: Northern Hemisphere teleconnection patterns during extreme phases of the zonal mean circulation. *J. Climate*, **9,** 2614–2633.

Trenberth, K. E., and G. W. Branstator, 1992: Issues in establishing causes of the 1988 drought over North America. *J. Climate*, **5,** 159–172.

——, and C. J. Guillemot, 1996: Physical processes involved in the 1988 drought and 1993 floods in North America. *J. Climate*, **9,** 1288–1298.

Wallace, J. M., and Q.-R. Jiang, 1987: On the observed structure of the interannual variability of the atmosphere/ocean climate system. *Atmospheric and Oceanic Variability*, H. Cattle, Ed., Roy. Meteor. Soc., 17–43.